A Highly Sensitive VEGF$_{165}$ Photoelectrochemical Biosensor Fabricated by Assembly of Aptamer Bridged DNA Networks

Huimei Da, Hongyan Liu, Yingning Zheng, Ruo Yuan, Yaqin Chai

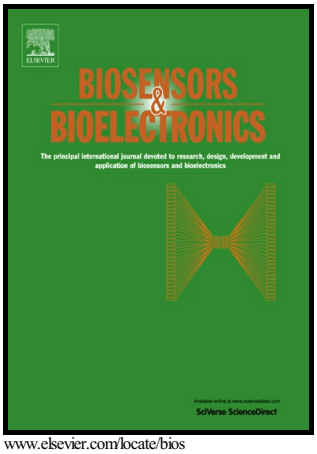

www.elsevier.com/locate/bios

PII: S0956-5663(17)30697-8
DOI: https://doi.org/10.1016/j.bios.2017.10.032
Reference: BIOS10057

To appear in: *Biosensors and Bioelectronic*

Received date: 24 August 2017
Revised date: 11 October 2017
Accepted date: 14 October 2017

Cite this article as: Huimei Da, Hongyan Liu, Yingning Zheng, Ruo Yuan and Yaqin Chai, A Highly Sensitive VEGF$_{165}$ Photoelectrochemical Biosensor Fabricated by Assembly of Aptamer Bridged DNA Networks, *Biosensors and Bioelectronic,* https://doi.org/10.1016/j.bios.2017.10.032

A Highly Sensitive $VEGF_{165}$ Photoelectrochemical Biosensor Fabricated by Assembly of Aptamer Bridged DNA Networks

Huimei Da, Hongyan Liu, Yingning Zheng, Ruo Yuan and Yaqin Chai**

Education Ministry Key Laboratory on Luminescence and Real-Time Analysis, College of Chemistry and Chemical Engineering, Southwest University, Chongqing 400715, People's Republic of China

liuhy860@swu.edu.cn

yaqinchai@swu.edu.cn

* Corresponding author. Tel.: +86-23-68252277; Fax: +86-23-68253172.

Abstract

We developed a novel "signal-off" photoelectrochemical (PEC) aptasensor based on an aptamer bridged DNA network structure for the sensitive detection of vascular endothelial growth factor ($VEGF_{165}$), using g-C_3N_4 as photoactive material. The DNA network provides an excellent platform for the immobilization of methylene blue (MB), which can facilitate the electron transport through the DNA helix structure and

suppress the recombination of electron-hole pairs generated by g-C_3N_4. In the presence of the target $VEGF_{165}$, the DNA network can be destroyed adequately by the recognition between $VEGF_{165}$ and the aptamer, resulting in the release of MB. Therefore, the originally enhanced electron transfer process could be inhibited, leading to a remarkable decrease of the photocurrent. A good linear relationship between the PEC signal and the logarithm of $VEGF_{165}$ concentration over the range of 100 fM to 10 nM with a detection limit of 30 fM can be obtained. Our concept can be easily extended to develop aptasensors for the sensitive detection of different targets by triggering the release of the payloads from their corresponding aptamer bridged DNA networks.

Keywords: $VEGF_{165}$; Photoelectrochemical; DNA Networks; signal-off

1. Introduction

Vascular endothelial growth factor ($VEGF_{165}$) is a substance produced by cells that simulates the formation of new blood vessels of tissues. (Itakura et al., 2008; Langer et al., 2000; Walsh et al., 1999) It is an important regulator of angiogenesis by activating the VEGF-receptor tyrosine kinases in endothelial cells. (Senger et al., 1983) $VEGF_{165}$ is also involved in osteogenesis and bone repair by stimulating survival, recruitment and migration of major bone forming cells. (Orlandini et al., 2006) However, the overexpression or down regulation of $VEGF_{165}$ is associated with

different diseases. For example, $VEGF_{165}$ is often over expressed in cancer cells during the tumor growth and influences the lymph-angiogenesis and the metastasis of cancers for the abnormally fast growth and division. (Loureiro et al., 2005) It has been reported to be an important biomarker for different diseases such as breast cancer, lung cancer, colorectal cancer, as well as rheumatoid arthritis. (Skobe et al., 2001) In this regard, the sensitive determination of the $VEGF_{165}$ can be a promising approach in clinical diagnoses for cancers. (Lee et al., 2009) Up to now, a variety of analytical platforms for the detection of $VEGF_{165}$ have been reported, such as ELISA assays, (Hsu et al., 2015) optical methods, (Kopra et al., 2014; Suzuki et al., 2009; Liu et al., 2017) surface plasmon resonance (SPR). (Liu et al., 2012) However, these methods are mainly time consuming, complex and expensive. Recently, aptamers have drawn widespread attention in the area of biosensors because of its advantages of high affinity, specificity, and stability compared to antibodies. (Potyrailo et al., 2015; Lee et al., 2015; Tran et al., 2013) Indeed, several aptamer-based biosensors for VEGF detection have been developed, including electrical field-effect transistor (FET) aptasensors, (Kwon et al., 2010; Kwon et al., 2012) electrochemical DNA aptasensors (Zhao et al., 2011) and optical aptasensors. (Freeman et al., 2012; Lin et al., 2016) However, the detection efficiency and sensitivity of these methods still require further improvement.

Photoelectrochemical (PEC) assay is a newly emerging and vibrantly developing analytical technique, which integrates both the advantages of optical and electrochemical method. (Wei et al., 2018) The PEC process refers to the photon-to-current conversion resulting from the charge separation and subsequent charge transfer of a photoactive material (usually organic or inorganic semiconductors) after absorbing photons upon illumination, and the formed electron-hole pairs at the interface would cause the oxidation-reduction reaction of the ground or excited states of molecules or ions to generate photocurrent. (Zhao et al., 2014) PEC assay has attracted much attention due to its unique properties such as low background noise, high sensitivity, easy operation and lower price. (Long et al., 2011; Cao et al., 2014) However, the detection of $VEGF_{165}$ by PEC method has been rarely reported. Therefore, it is desired to propose a PEC aptasensor for $VEGF_{165}$ with rapid detection and high sensitivity.

The "signal-off" model was a very classic and convenient signal response pattern for construction of PEC biosensors. Generally, in "signal-off" type PEC biosensors, an efficient photocurrent signal quencher with ideal quenching efficiency for the initial photocurrent of photoactive materials are necessary. However, the development of PEC biosensor was still in its infancy, it was very difficult and time consuming to search for a proper signal quencher with excellent quenching effect for the photocurrent signal of special photoactive materials. (Zang et al., 2014; Li et al.,

2016) Therefore, it is highly significant but full of challenges to develop a more convenient and effective "signal-off" model in PEC biosensor which could be applied to quench the photocurrent of majority of the photoactive materials. Recently, DNA nanotechnology provides new opportunities for the design of biosensor. The assembly of propagating structures through DNA hybridization paves the way for the engineering of 3D DNA films with tailored composition, structure, and permeability, making them likely to find application in drug/gene delivery and biomolecular sensing. (Lu et al., 2015; Liao et al., 2016) Inspired from this unique structure, it is possible to develop PEC DNA sensing platforms by assembly of the DNA layer on an electrode to form 3D DNA networks. Since there are pores and double strand DNA (dsDNA) platforms in the 3D networks, different payloads such as photoactive materials, sensitizer and quencher can be entrapped and immobilized. By the incorporation of a sequence specific aptamer into the DNA networks and the opening of the networks by the formation of aptamer-ligand complexes, the PEC signal should altered by trigger the release of the payloads entrapped in the DNA networks.

Herein, we developed a novel "signal-off" PEC aptasensor based on assembly and disassembly of an aptamer bridged 3D DNA network structure for the sensitive detection of $VEGF_{165}$. Graphitic carbon nitride (g-C_3N_4), a metal-free photoactive semiconductor with desirable photo-to-current conversion efficiency, was employed as a photocurrent signal material to provide an initial photocurrent signal in this work. As

shown in Scheme 1, two different motifs (D1 and D2) were immobilized on the g-C_3N_4 modified electrode to obtain the first DNA layer. By repeating this process, the $VEGF_{165}$ aptamer bridged DNA networks can be assembled. The DNA network provides an excellent dsDNA platform for the incorporation of methylene blue (MB), a redox-active intercalator that can improve the conductivity of DNA, thus facilitating the electron transport through its helix structure and further enhance the PEC signal. In the presence of the $VEGF_{165}$, the DNA network can be destroyed through the formation of aptamer-$VEGF_{165}$ complex, resulting in the release of MB, which further induces a decrease of the PEC signal (Scheme 1). A linear relationship between the PEC signal and the logarithm of $VEGF_{165}$ can be obtained. Thus, we developed a new recognition pattern to achieve the sensitive and specific detection of $VEGF_{165}$.

2. Experiment

2.1 Chemicals and material

Methylene blue (MB) was purchased from Shanghai Aladdin Industrial Corporation (Shanghai, China). H_2O_2 and Melamine were purchased from Kelong Chemical Inc. (Chengdu, China). Hexanethiol (HT) and Gold chloride ($HAuCl_4$) were supplied by Sigma Chemical Co. (St. Louis. MO, USA). $K_3[Fe(CN)_6]$ and $K_4[Fe(CN)_6]$ were bought from Beijing Chemical Reagent Co. (Beijing, China). Tris-

hydroxymethylaminomethane-hydrochloride (Tris) was purchased from Shanghai. Roche Pharmaceutical Ltd. (Shanghai, China). $VEGF_{165}$ was bought from Shanghai Sangon Biological Engineering Technology and Services Co., Ltd. (Shanghai, China).

20 mM Tris-HCl solution (pH 7.4) consisting of 1 mM CaCl2, 1 mM MgCl2, 5 mM KCl and 140 mM NaCl was utilized for diluting DNA. 0.1 M phosphate buffer solutions (PBS) (pH 7.4) including 0.1 M KCl was used throughout the experiment. $[Fe(CN)_6]^{3-/4-}$ solution (pH 7.4, 5.0 mM) was prepared by dissolving potassium ferricyanide and potassium ferrocyanide in PBS solution (pH 7.4). All chemicals were of analytical grade. Ultrapure water was used throughout the experiments.

The oligonucleotides sequences were bought from Shanghai Sangon Biological Engineering Technology and Services Co., Ltd. (Shanghai, China). The sequences were listed as follows:

S_0: 5'-SH-CCCCCCCCCCATAGTAGTTCCGTC-3'

S_1: 5'-CTACTATAATGACGGAA-3'

S_2:

5'-ATAGTAGTTCCGTCTTCCAGACAAGAGTGCAGGGTATAAGAAT-3'

S_3: 5'-TACCCTGTAAATTCTTA-3'

2.2 Apparatus and characterization

The PEC measurements were carried out with a PEC workstation (Ivium, Netherlands). Cyclic voltammetry (CV) were realized with a CHI 660e electro-chemistry workstation (Shanghai Chenhua Instrumission, China). The morphologies of the prepared nanomaterials were characterized by transmission electron microscope (TEM, JEM-2100). UV-visible (UV-vis) absorption spectrums were carried out on UV-2450 UV-vis spectrophotometer (Shimadzu, Tokyo, Japan). A three-electrode system composed of a platinum wire were used as the counter electrode, an Saturated Calomel Electrode (SCE, saturated KCl) as the reference electrode and a glassy carbon electrode (GCE, Φ = 4 mm) as the working electrode.

2.3 Synthesis and characterization of g-C_3N_4

The g-C_3N_4 was synthesized according to the previously reported method with minor modification. (Zhang et al., 2012) 5g Melamine in a crucible with a cover under ambient pressure in air was dried at 80 ^oC for 24 h, followed by calcination in a muffle furnace at 550 ^oC for 3 h with a heating rate of 5 ^oC min^{-1} to complete the reaction. The prepared samples were powders with a nlight yellow color. Finally, the powders were washed with nitric acid (0.1 M) and distilled water to remove any residual alkaline species (e.g. ammonia) adsorbed on the sample surface. (De Pablo et al., 2000)

2.4 Preparation of the PEC aptasensor for $VEGF_{165}$ assay

Primarily, the bare GCE was polished with alumina slurry and sonicated in ultrapure water for a completely clean surface. 15 μL of g-C_3N_4 (2 mg mL^{-1}) was then dropped onto the surface of electrodes. After drying at 37 °C, the electrodes were coated with Au NPs by electrotrolytic deposition under a constant potential of -0.2 V for 5 s. Subsequently, the electrodes were incubated with 10 μL of 1 μM S_0 at 4 °C for 12 h and blocked with 20 μL of 0.1 mM HT for 40 min. The mixture of 10 μL of 2 μM S_1 and 10 μL of 1 μM S_2 was denoted as D1. As show in Scheme 1, 20 μL D1 was dropped onto the modified electrodes and incubated at room temperature for 2 h to hybridize with S_0 and to yield the first DNA layer. The mixture of 10 μL of 1 μM S_2 and 10 μL of 2 μM S_3 was denoted as D2. The obtained electrodes were incubated with 20 μL D2 to yield the second DNA layer. By repeating D1 and D2, four layers of DNA can be assembled on the electrodes, which were bridged by the S_2 that including the $VEGF_{165}$ aptamer sequence. After 5 μL of 0.4 mM MB was dropped onto the modified electrodes, a higher PEC singal can be obtained, as shown in Scheme 1 ("without target" curve). Finally, $VEGF_{165}$ with different concentrations were incubated with the modified electrodes at room temperature for 1 h, the PEC signal was decreased, as show in Scheme 1 ("target" curve).

3. Results and discussion

3.1 Morphology and spectroscopic characterizations of C_3N_4

The g-C_3N_4 was used as photoactive material for the PEC aptasensor. The as-prepared g-C_3N_4 was characterized with TEM and UV-vis measurement. As shown in Fig. S1, the TEM image shows a two dimensional sheet structure with a wrinkle surface. A typical porous morphology of g-C_3N_4 can be clearly observed. The UV-Vis absorption spectrum of g-C_3N_4 is presented in Fig. S2. The spectrum reveals a strong absorption peak at 303 nm with a range from 300 to 500 nm, indicating a good light harvesting in the region of the visible spectrum.

3.2 Characterization of the proposed biosensor

PEC and CV measurements were used to monitor the stepwise fabrication process of the electrode. Fig. 1A shows the photocurrent of different modified electrodes. As displayed by curve a, no photocurrent response was observed for the bare GCE. With the modification process of g-C_3N_4, the photocurrent increased conspicuously, provide a basic PEC signal for the biosensor (curve b). AuNPs, S_0 and HT were then introduced successively (curve c, d and e, respectively), the photocurrents of the electrodes modified by AuNPs were increased due to the surface plasmonic resonance (SPR) phenomenon in metallic nanostructures, the photocurrents of the electrodes modified by S_0 and HT were declined due to the inhibition effect of

DNA and HT. Subsequently, 3D DNA network including $VEGF_{165}$ aptamer was assembled on the modified electrode by repeating the immobilization of D1, D2 and D1(curve f, g and h). Afterwards, with addition of the mixture solution including D2 and MB, the photocurrent increased rapidly (curve i), this is probably because of the MB was embedded in DNA duplex that could improve the electron transfer efficiency of g-C_3N_4, increase the utilization of light energy, and facilitate the charge separation effectively. (Gill et al., 2005) Finally, the photocurrent decreased evidently after 10 nM $VEGF_{165}$ was added (curve j), it could be attributed to the realease of MB from the electrode, (Liao et al., 2016) the originally enhanced electron transfer process could be inhibited, leading to a remarkable decrease of the photocurrent. However, the increase of the PEC signal induced by the release of DNA is minor, which is far below the decrease of the photocurrent induced by the release of MB. Therefore, the photocurrent decreased after adding of $VEGF_{165}$. The stepwise fabrication process of the biosensor was also investigated by CV measurements. As shown in Fig. 1B and C, a couple of well-defined $[Fe(CN)_6]^{3-/4-}$ redox peak could be acquired at a bare GCE (curve a), whereas redox peak decreased was observed after modified with g-C_3N_4 (curve b). The redox peak current was increased after AuNPs were introduced due to effectively promote electron transfer (curve c). When S_0 and HT were introduced in turn, the redox peak current was decreased (curve d and e) due to the inhibition of electron transfer from the DNA and HT, which is also convinced by the decrease of

the peak value after the DNA layer was assembled on the electrode surface (curve f, g and h). The redox peak increased after the electrode was incubated with D2-MB, this is mainly attributed to the effective sensitization of MB (curve i). Finally, the redox peak evidently decreased because of the interaction of the aptamer and $VEGF_{165}$ that forming hairpin structure, leading to the release of MB from the electrode surface (curve j).

The photocurrent generating mechanism and the electron transfer steps of the g-C_3N_4 materials sensitized by MB is shown in Scheme 1. DNA usually exhibits poor conductivity and hence acts as an inefficient charge transporter for the electrons. (Lee et al., 2010) MB is a redox active species as mediator to shuttle electron along the DNA double helix. Therefore, MB was incorporated into the dsDNA to improve the conductivity of DNA, it can also increase the utilization of light energy and facilitate the charge separation, resulting in enhancement of the photocurrent conversion efficiency. (Willner et al., 2001; Gill et al., 2005; Freeman et al., 2007) Under the light irradiation, electrons and holes are generated in the conduction band (CB) and valence band (VB) of g-C_3N_4, respectively. There are two major flow directions for the generated electron-hole pairs. One is electron-hole recombination, which decreased the

photocurrent response of the aptasensor, and the other was the electron transfer and charge separation, which enhanced the photocurrent response of the aptasensor. In the PEC measurements, H_2O_2 was used as an electron donor. In the absence of MB, the electron-hole recombination process was the dominant, whereas greatly inhibited the electron transfer process, leading to a low signal response. In the presence of MB, the charge separation efficiency of the g-C_3N_4 could be significantly enhanced, resulting in a high photocurrent response. Finally, in the presence of the target $VEGF_{165}$, MB could be released from the DNA network because of the recognition of aptamer and $VEGF_{165}$. Therefore, the originally electron transport process would be inhibited, leading to a remarkable decrease of the photocurrent value, as shown in Scheme 1. Thus, a ‘‘signal off’’ PEC aptasensor can be constructed for the quantitative detection of target $VEGF_{165}$.

The formed DNA network structure was also characterized by polyacrylamide gel electrophoresis (PAGE). As show in Figure. S3, the distinct bands from lanes 1-3, respectively, correspond to the three single strands (S1, 17nt; S2, 43nt, S3, 17nt). It can be observed that lane 2 posed a higher position comparing with S1 (lane 1) and S3 (lane 3). Further incubation of D1 and D2, led to the appearance of lane 4 with lower mobility, suggesting the DNA network structure were probably formed.

3.3 Optimization of experimental conditions for the fabrication of aptasensor

MB was used to improve the conductivity of DNA and facilitate the charge separation. Therefore, the concentration of MB is an important influence factor for the sensitivity of the PEC biosensor. Therefore, the effect of MB concentration on the photocurrent intensity was investigated. As shown in Fig. S4A, the photocurrent successively increased until 0.43 mM and then decreased, indicating that 0.43 mM was the optimal MB concentration. In addition, H_2O_2 was used as an electron donor in the PEC measurements. Thus, the effect of H_2O_2 on the photocurrent intensity was also investigated. As shown in Fig. S4B, the photocurrent was increased remarkably with the increasing of H_2O_2, which attribute to the fact that H_2O_2 could improve the charge separation and further enhance the photocurrent intensity. The concentration of H_2O_2 used in this study was 0.1 M.

3.4 Sensitivity of the aptasensor

The photoelectrochemical $VEGF_{165}$ detection was based on the release of MB from DNA network after the aptamer specifically binding with $VEGF_{165}$. Therefore, the photocurrent response was directly related to the concentration of $VEGF_{165}$. The proposed aptasensor was investigated after the interaction with various concentrations of $VEGF_{165}$. As shown in Fig. 2A, the photocurrent decreased with increasing of

$VEGF_{165}$ concentration. The quantitative behavior between the photocurrent and the concentration of $VEGF_{165}$ is confirmed, as shown in Fig. 2B, the PEC biosensor showed a linear relationship between photocurrent and the logarithm of $VEGF_{165}$ concentrations in the range from 100 fM to 10 nM. The linear regression equation was I = -0.2521lg$c$ +1.9141 with a correlation coefficient of 0.9902. In addition, the detection limit was 0.03 pM at the signal-to-noise ratio of 3, which is much lower than the previously reported results as summarized in Table 1. The present PEC biosensor showed high sensitivity and wide linear range for the sensitive detection of $VEGF_{165}$.

3.5 Stability and selectivity of the PEC aptasensor

Detection specificity and stability are important concerns for biosensors. To investigate the stability, the proposed aptasensor was therefore used in the analysis of $VEGF_{165}$ (1 nM) under periodic off-on-off light for 9 cycles. As shown in Fig.3A, the photocurrent showed no severe decay in repeated experiments, suggesting an excellent stability. To prove the detection specificity of the developed biosensor, the photocurrent change of different interaction models, L-Cysteine (L-Cys), thrombin (TB), hemoglobin (Hb), Bovine serum albumin (BSA) and human immunoglobulin (lgG) was investigated. As shown in Fig. 3B, the addition of 10 nM of $VEGF_{165}$

resulted in an obvious photocurrent decrease (ΔI=0.962 μA), whereas an addition of 100 nM of L-Cys, TB, Hb, BSA and lgG generated negligible photocurrent changes (ΔI=0.137 μA, 0.105 μA, 0.193 μA, 0.121 μA, 0.101 μA respectively). The differences between the electrodes with different interaction proteins were obvious. Therefore, it is reasonable to conclude that the proposed PEC aptasensor displayed high specificity to $VEGF_{165}$.

4 Conclusions

We described a novel "signal-off" PEC aptasensor that can achieve the sensitive detection of $VEGF_{165}$. By using g-C_3N_4 as photoactive materials, the PEC assay was developed based on assembly and disassembly of an aptamer bridged DNA network structure incorporated by MB. In the presence of the $VEGF_{165}$, the release of MB from the DNA networks induced a decrease of the photocurrent, which provided an analytical signal for $VEGF_{165}$. The results demonstrated that the proposed PEC assay could offer high specificity, sensitivity, and stability for the detection of $VEGF_{165}$. The excellent properties endow the PEC aptasensor very broad applications in clinical diagnoses for cancers. The assembly and disassembly method provided a new concept for the fabrication of "signal-off" PEC biosensor. It can be easily extended to develop

other highly efficient and stable biosensors to recognize different biomarkers of vital diseases.

Acknowledgements

This work was financially supported by the National Natural Science Foundation of China (21501081, 21575116, 21473136) and the Fundamental Research Funds for the Central Universities (XDJK2017C021).

References

Cao, H. J., Liu, S. S., Tu, W. W., Bao, J. C., Dai, Z. H., 2014. Chem. Commun. 50, 13315–13318.

De Pablo, P. J., Moreno-Herrero, F., Colchero, J., 2000. Phys. Rev. Lett. 85, 4992–4995.

Freeman, R., Girsh, J., Fang-ju Jou, A., Ho, Ja.A., Hug, T., Dernedde, J., Willner, I., 2012. Anal. Chem. 84, 6192–6198.

Freeman, R., Gill, R., Beissenhirtz, M., Willner, I., 2007. Photochem. Photobiol., Sci. 6, 416–422.

Gill, R., Patolsky, F., Katz, E., Willner, I., 2005. Angew. Chem. Int. Ed. 44, 4554–4557.

Hsu, M. Y.,Chen,S. J.,Chen, K. H., Hung, Y. C.,Tsai, H. Y.,Cheng, C. M.,2015. Lab Chip. 15, 2357–2363.

Itakura, E., Yamamoto, H., Oda, Y., Tsuneyoshi, M., 2008. J. Surg. Oncol. 97, 74–81.

Jang, J., 2012. ACS Nano. 6, 1486–1493.

Kopra, K., Syrjanpaa, M., Hanninen, P., Harma, H., 2014. Analyst.139,2016–2023.

Kwon, O. S., Park, S. J., Jang, J., 2010. Biomaterials. 31, 4740–4747.

Kwon, O. S., Park, S. J., Hong, J. Y., A-Reum, H., Lee, J. S.,James S. Lee, Oh, J. H.,

Langer, I., Vertongen, P., Perret, J., Fontaine, J., Atassi, G., Robberecht, P., 2000. Med. Pediatr. Oncol. 34, 386–393.

Lee, H. S., Kim, K. S., Kim, C. J., Hahn, S. K., Jo, M. H., 2009. Biosens. Bioelectron. 24, 1801–1805

Lee, S. E., Chen, Q., Bhat, R., Petkiewicz, S., Smith, J. M., Ferry, V. E., Correia, A. L., Alivisatos, A. P., Bissell, M. J., 2015. Nano Lett. 15, 4564–4570.

Lee, Y. L., Chi, C. F., Liau, S. Y., 2010. Chem. Mater. 22, 922–927.

Liao, W. C., Sohn, Y. S., Riutin, M., Cecconello, A., Parak, Wolfgang J., Nechushtai, R., Willner, I., 2016. Adv. Funct. Mater. 24, 4262–4273.

Li, M. J., Zheng, Y. N., Liang, W. B., Yuan, Y. L.,Chai, Y. Q., Yuan, R., 2016. *Chem. Commun.* 52, 8138–8141.

Lin, X. X., Leung, K. H., Lin, L., Lin, L. Y., Lin, S., Leung, C. H., Ma, D. L., Lin, J. M., 2016. Biosens. Bioelectron. 79, 41–47.

Liu, C., Lei, T., Ino, K., Matsue, T., Tao, N., Li, C. Z., 2012. Chem.Commun. 48, 10389–10391.

Liu, C. F., Yang, C ., Lu, L. H., Wang, W. H., Tan, W. H., Leung, C. H., Ma, D. L., 2017. Chem. Commun. 53, 2822-2825

Long, Y. T., Kong, C., Li, D. W., Li, Y., Chowdhury, S., Tian, H., 2011. Small. 7, 1624–1628.

Loureiro, R. M., D′Amore, P. A., 2005. Cytokine Growth Factor Rev. 16, 77–89.

L., Alitalo, K., Claffey, K., Detmar, M., 2001. Nat. Med. 7, 192 – 198.

Lu, C. H., Willner, I., 2015. Angew. Chem. Int. Ed. 54, 12212–12235.

Orlandini, M., Spreafico, A., Bardelli, M., Rocchigiani, M., Salameh, A., Nucciotti, S., Capperucci, C., Frediani, B., Oliviero, S., 2006. J. Biol. Chem. 281, 17961–17967.

Potyrailo, R. A., Murray, A. J., Nagraj, N., Pris, A. D., Ashe, J. M., Todorovic, M., 2015. Angew. Chem. Int. Ed. 54, 2174–2178.

Prabhulkar, S., Alwarappan, S., Liu, G., Li, C. Z., 2009. Biosens. Bioelectron. 24, 3524–3530.

Senger, D. R., Galli, S. J., Dvorak, A. M., Perruzzi, C. A., Harvey, V. S., Dvorak, H. F., 1983. Science. 219, 983–985.

Skobe, M., Hawighorst, T., Jackson, D. G., Prevo, R., Janes, L., Velasco, P., Riccardi, L., Alitalo, K., Claffey, K., Detmar, M., 2001. Nature Medicine. 7, 192 – 198.

Suzuki, Y., Yokoyama, K., 2009. ChemBioChem. 10, 1793–1795.

Tran, T. N. N., Cui, J. H., Hartman, M. R., Peng, S., Funabashi, H., Duan, F., Yang, D. Y., March, J. C., Lis, J. T., Cui, H.X., Luo. D., 2013. J. Am. Chem. Soc. 135, 14008-14011.

Walsh, K., Sherwood, R. A., Dew, T. K., Mulvin, D., 1999. BJU Int. 84, 1081–1083.

Wei, Y. B, .Zeng, Q., Hu, Q., Wang, M., Tao, J., Wang, L. S., 2018. Biosens. Bioelectron. 99, 136-141.

Willner, I., Patolsky, F., Wasserman, J., 2001. Angew. Chem. Int. Ed. 40, 1861–1864.

Zang, Y., Lei, J. Q., Hao, Q., Ju, H. X., 2014. ACS Appl. Mater. Interfaces. 6, 15991-15997

Zhang, Y. W., Liu, J. H., Wua, G., Chen, W., 2012. Nanoscale. 4, 5300–5303.

Zhang, H., Li, M. X., Li, C. H., Guo, Z. H., Dong, H. L., Wu, P., Cai, C. X., 2015. Biosens. Bioelectron. 74, 98–103.

Zhao, J., Hea, X., Bo, B., Liu, X., Yin, Y., Li, G., 2012. Biosens. Bioelectron. 34, 249–252.

Zhao, S., Yang, W., Lai, R. Y., 2011. Biosens. Bioelectron. 26, 2442–2447.

Zhao, W. W., Xu J. J., Chen, H. Y., 2014. Chem. Rev. 114, 7421–7441.

Scheme 1. Schematic illustration for the preparation and mechanism of the PEC aptasensor

Figure 1. PEC response (A) and CV response (B) of (a) bare GCE, (b) C_3N_4/GCE, (c) Au/C_3N_4/GCE, (d) S_0/Au/C_3N_4/GCE, (e) HT/S_0/Au/C_3N_4/GCE, (f) D1/HT/S_0/Au/C_3N_4/GCE, (g) D2/D1/HT/S_0/Au/C_3N_4/GCE, (h) D1/D2/D1/HT/S_0/Au/C_3N_4/GCE, (i) D2-MB/D1/D2/D1/HT/S_0/Au/C_3N_4/GCE, (j) $VEGF_{165}$/D2-MB/D1/D2/D1/HT/S_0/Au/C_3N_4/GCE; (C) Magnification of one segment of the (B).

Figure 2. (A) Photocurrent response of the aptasensor at different concentrations of $VEGF_{165}$: 100 fM (a), 1 pM (b), 10 pM (c), 100 pM (d), 1 nM (e), 10 nM (f). (B) The corresponding linear calibration curve.

Figure 3. (A) Stability of the PEC aptasensor under periodic light for 9 cycles. (1 nM $VEGF_{165}$). (B) Selectivity of the PEC aptasensor to $VEGF_{165}$ by comparing it to the 10-fold excess of other interfering substances.

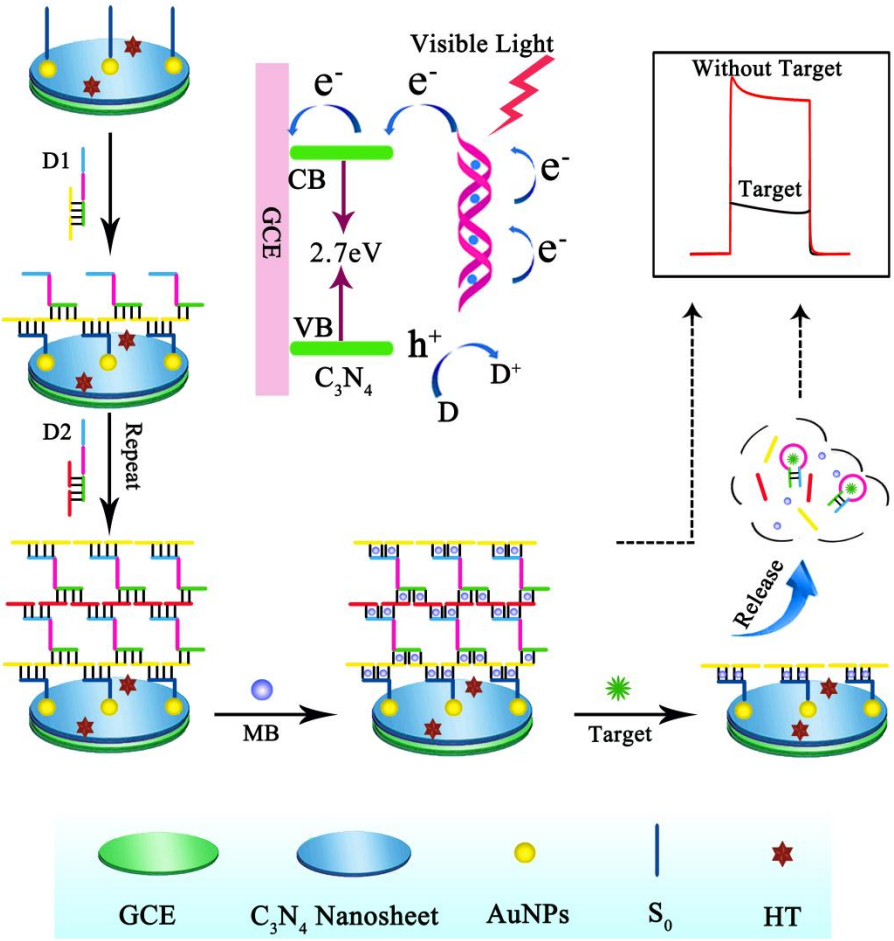

Scheme 1

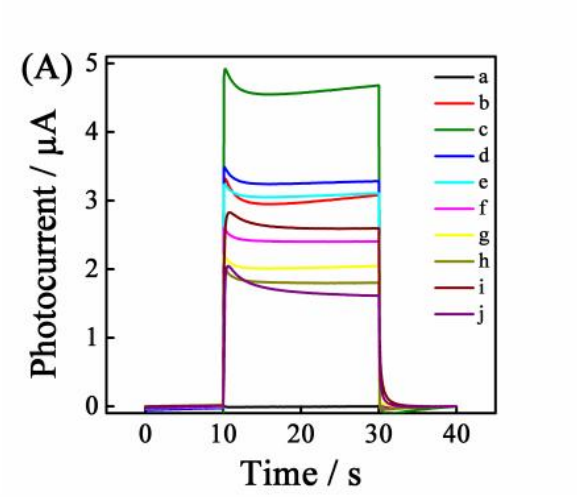
(A)
Photocurrent / μA
Time / s
a
b
c
d
e
f
g
h
i
j

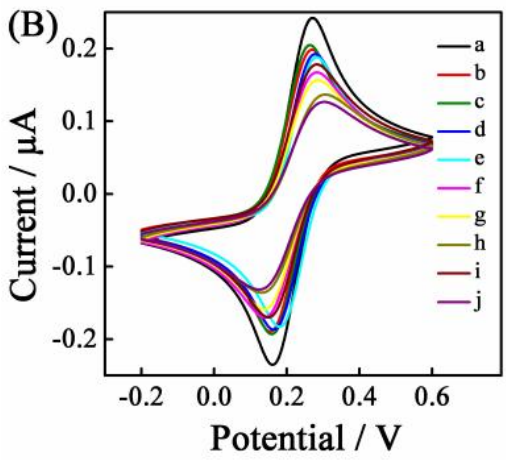
(B)
Current / μA
Potential / V
a
b
c
d
e
f
g
h
i
j

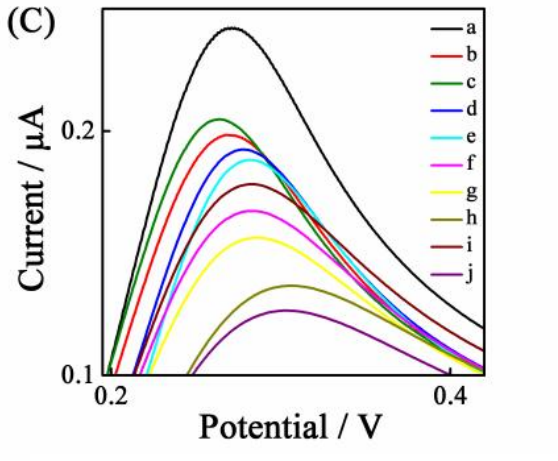
(C)
Current / μA
Potential / V
a
b
c
d
e
f
g
h
i
j

Figure 1

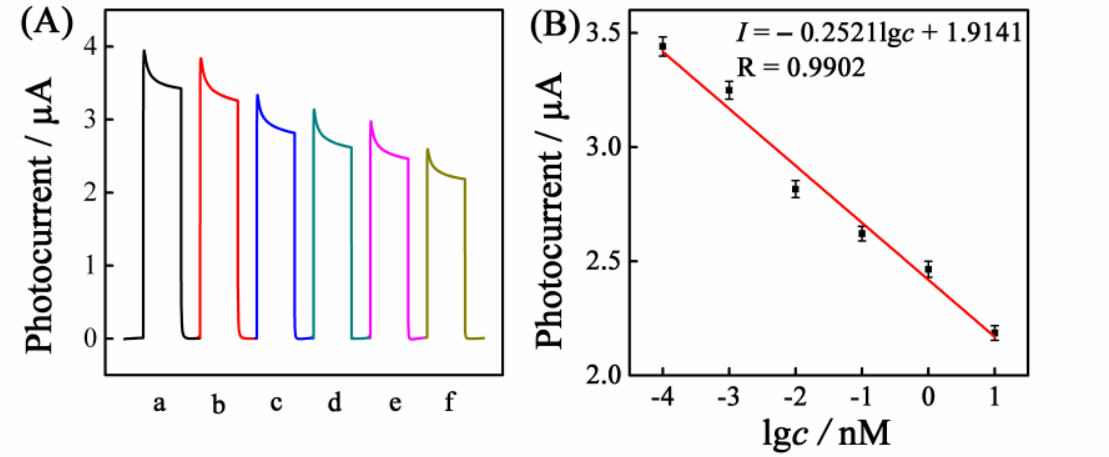

Figure 2

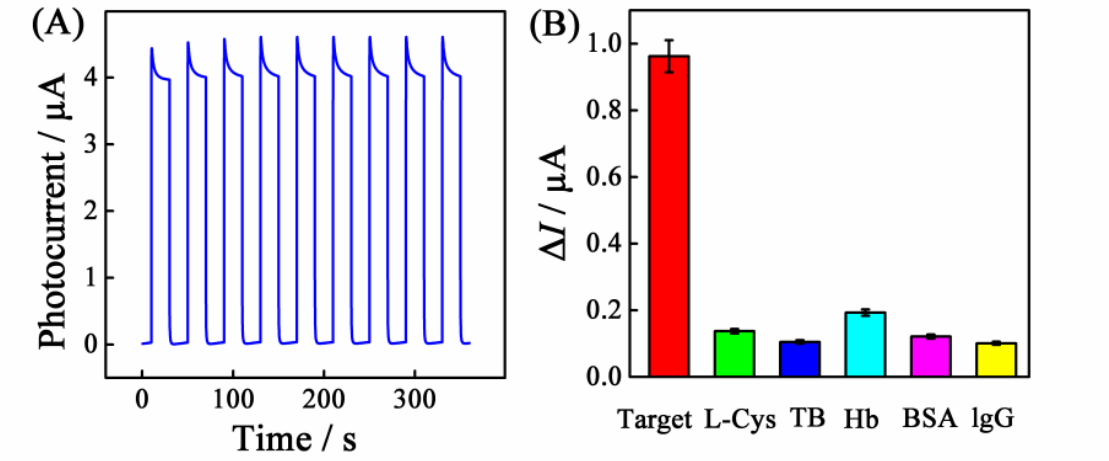

Table 1. Comparison of the analytical performance of the different $VEGF_{165}$ sensors.

Analytical method	Linear range (pM)	Detection limit (pM)	Ref.
ECL	$1–20\times10^3$	0.2	Zhang et al., 2015
Fluorescence	0.52–52	–	Lin et al., 2016
FET	1.04–104	–	Lee et al., 2009
Optical	–	50	Ronit Freeman et al.,2012
SWV	$1\times10^3–20\times10^3$	–	Zhao et al., 2012
PEC	$0.1–1\times10^4$	0.03	This work

Abbreviations: electrochemiluminescent (ECL); fluorescence (FL); field-effect transistor (FET); square-wave voltammetry (SWV).

Highlights

- A novel "signal-off" photoelectrochemical (PEC) aptasensor based on an aptamer bridged DNA network structure.

- This strategy was utilized in a PEC aptasensor for the detection of $VEGF_{165}$ with high specificity, sensitivity, and stability.

- The method can be easily extended to develop aptasensors for the sensitive detection of different targets by triggering the release of the payloads from their corresponding aptamer bridged DNA networks.